

Acta Crystallographica Section C

**Crystal Structure
Communications**

ISSN 0108-2701

Editor: **George Ferguson**

$\text{Al}_6\text{Ti}_2\text{O}_{13}$, a new phase in the $\text{Al}_2\text{O}_3\text{--TiO}_2$ system

Stefan T. Norberg, Stefan Hoffmann, Masahiro Yoshimura and Nobuo Ishizawa

Copyright © International Union of Crystallography

Author(s) of this paper may load this reprint on their own web site provided that this cover page is retained. Republication of this article or its storage in electronic databases or the like is not permitted without prior permission in writing from the IUCr.

Al₆Ti₂O₁₃, a new phase in the Al₂O₃–TiO₂ system

Stefan T. Norberg,^{a*} Stefan Hoffmann,^b Masahiro Yoshimura^b and Nobuo Ishizawa^a

^aCeramics Research Laboratory, Nagoya Institute of Technology, 10-6-29 Asahigaoka, Tajimi, Gifu 507-0071, Japan, and ^bMaterials and Structures Laboratory, Tokyo Institute of Technology, 4259 Nagatsuta Midori, Yokohama 226-8503, Japan
Correspondence e-mail: stn@crl.nitech.ac.jp

Received 21 December 2004

Accepted 24 January 2005

Online 28 February 2005

The compound Al₆Ti₂O₁₃ (hexaaluminium dititanium tridecaoxide) has been synthesized using an arc-imaging furnace, which allows fast cooling of melted oxides. The structure consists of infinite double chains of polyhedra running along the *c* axis. These chains are built up by four kinds of strongly distorted oxygen octahedra randomly occupied by either Ti or Al (point symmetry *m* or *m2m*), and by trigonal bipyramids exclusively occupied by Al (point symmetry *m2m*).

Comment

The structural examination of the titanium suboxides with the general formula Ti_{*n*}O_{2*n*-*p*} (where *n* and *p* are positive integers) led to the evolution of the principle of crystallographic shear as an underlying structural principle (Hyde & Andersson, 1989). This concept is devoted to the question of how structures with similar stoichiometry are related (Gibb & Anderson, 1972*b*). After the validation of this concept for titanium oxides by means of transmission electron microscopy (TEM) and single-crystal X-ray diffraction, the investigations were extended to pseudo-binary systems, M₂O₃–TiO₂, where M₂O₃ denotes an oxide of a trivalent cation with an ionic radius similar to Ti⁴⁺, e.g. Cr³⁺ (Bursill *et al.*, 1971; Gibb & Anderson, 1972*a*) and Fe³⁺ (Gibb & Anderson, 1972*b*).

Nevertheless, little attention has been paid to the phase system Al₂O₃–TiO₂, in which only one compound is known, namely β-Al₂TiO₅ (Austin & Schwartz, 1953), which adopts the pseudobrookite (Pauling, 1930) structure type. This compound has been studied extensively because of its physical properties. As a result of its low thermal expansion (Bayer, 1971, and references therein), it has, for instance, found a number of commercial applications with major European motor manufacturers as exhaust port liners in both petrol and diesel engines as a means of improving thermal efficiency. It is also under serious consideration for use in exhaust manifold inserts, piston crowns and turbocharger liners. Additionally, it finds application in non-ferrous metallurgical industries

(Thomas & Stevens, 1989). Later TEM investigations of Al₂O₃–TiO₂ samples with 50–70 mol% Al₂O₃ (Mazerolles *et al.*, 1994) revealed new phases with *c* axes of 12.4 and 16.8 Å, respectively, that were deemed by electron diffraction patterns to be structurally related to β-Al₂TiO₅.

Our research interest regarding high refractory oxides (Kamiya *et al.*, 1980; Yashima *et al.*, 1993) led us to the reinvestigation of the Al₂O₃–TiO₂ system using an arc-imaging furnace. This method of preparation ensures the complete melting of the oxides, avoiding the diffusion problems often observed in solid-state reactions, as well as reactions with the crucible material. In the course of these experiments, we were able to synthesize homogenous samples of the title novel compound suitable for single-crystal X-ray diffraction. The stoichiometry of the investigated sample was confirmed to be Al₆Ti₂O₁₃, as indicated from an energy-dispersive X-ray diffraction study of multiple crystalline fragments.

The structure of the title compound was solved and refined in space group *Cm2m*. There are five crystallographically independent metal (*M*) atomic sites and eight O atomic sites in the unit cell. Three of the *M* sites have point symmetry *m*, while the other two have point symmetry *m2m*. One of the *M* sites with point symmetry *m2m* is situated in a trigonal bipyramid of O atoms. The population refinement indicated that this site is wholly occupied by Al, and it is herein denoted Al1. The remaining *M* sites, named M2, M3, M4 and M5, are all located in distorted oxygen octahedra and are populated with both Ti and Al, in the proportions $\frac{2}{7}$ Ti and $\frac{5}{7}$ Al.

It should be noted that the refinement of the occupancies of the M2–M5 sites individually gave results that were either within experimental error of the $\frac{2}{7}$ Ti: $\frac{5}{7}$ Al ratio, or were so highly correlated with the displacement parameters as to be unreliable. Consequently, it was decided to fix the occupancies of these sites to be the same. Small variations from this Ti:Al ratio among the different sites cannot be ruled out.

The rather high residual electron density prompted us to carry out a thorough examination of all electron-density features (especially near the highest peaks). The residual electron density displayed in Fig. 1(*a*) illustrates typical electron features found on the mirror planes, while the rest of the

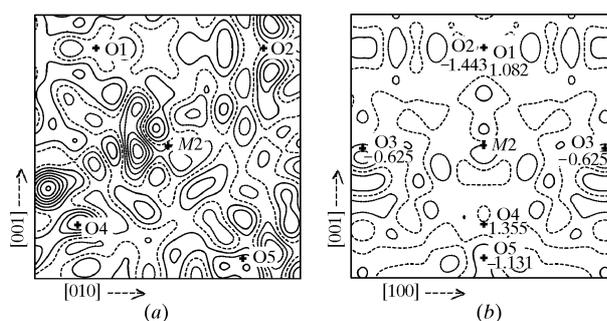


Figure 1

$\Delta\rho$ maps for Al₆Ti₂O₁₃, with positive and negative contours as solid and dotted lines, respectively, at increments of $0.4 \text{ e } \text{\AA}^{-3}$ [$\sigma(\Delta\rho) = 0.20 \text{ e } \text{\AA}^{-3}$]. The zero contours are dashed and the numbers indicate the distance of the atomic position from the viewed plane. (*a*) The slightly chaotic residual electron density in the mirror plane as centred on M2, compared with (*b*), which is also centred on M2.

structural model is free from high peaks of residual electron density, *e.g.* Fig. 1(b). The $2.8(2) \text{ e } \text{ \AA}^{-3}$ peak located $0.709(8) \text{ \AA}$ from atom O4 is the most pronounced, while another electron-density peak of $2.5(2) \text{ e } \text{ \AA}^{-3}$ is positioned $0.4993(2) \text{ \AA}$ from the Al1 site. The electron-density holes follow the same pattern as the peaks, with the largest hole of $-2.3(2) \text{ e } \text{ \AA}^{-3}$ located $0.455(5) \text{ \AA}$ from the M2 site.

It is not totally unexpected to find some rather high peaks of residual electron density, as $\text{Al}_6\text{Ti}_2\text{O}_{13}$ samples in general should be likely to contain intergrowths of related compounds. High-resolution TEM studies of Al-enriched $\beta\text{-Al}_2\text{TiO}_5$ crystals (Mazerolles *et al.*, 1994) showed intergrowth between $\beta\text{-Al}_2\text{TiO}_5$, the present $\text{Al}_6\text{Ti}_2\text{O}_{13}$ and still another phase of unknown composition. This was indicated as an observation of two unknown materials with *c* axes of 12.4 \AA and 16.8 \AA . The former probably corresponds to the structure analysed in the present study. The latter may correspond to an as yet unknown structure with a composition richer in Al. It is therefore possible that a small amount of intergrowth with $\beta\text{-Al}_2\text{TiO}_5$ and/or the still unknown Al-richer compound is present in the crystal studied here.

The arrangement of atoms in the new structure, $\text{Al}_6\text{Ti}_2\text{O}_{13}$, is shown in Fig. 2. Viewing the atomic lattice along the *c* axis reveals layers of atoms which are separated by $b/2$, and each layer is further divided into infinite double strings consisting of metal and O atoms, as seen in Fig. 3. These double strings can be regarded as the equatorial plane of a double chain of polyhedra of the same height, as shown in Fig. 4. Four different types of distorted octahedra and one type of trigonal bipyramid are connected by common edges and apices. The centres of all four octahedra are occupied by both Al^{3+} and Ti^{4+} ions, whereas the trigonal bipyramid is exclusively centred by Al^{3+} ions (the Al1 site). The metal–oxygen distances within the octahedra range between $1.790(8) \text{ \AA}$ (M4–O7) and $2.093(8) \text{ \AA}$ (M3–O6), while they range more tightly between $1.789(8) \text{ \AA}$ (Al1–O1) and $1.936(6) \text{ \AA}$ (Al1–O3) for the trigonal bipyramid.

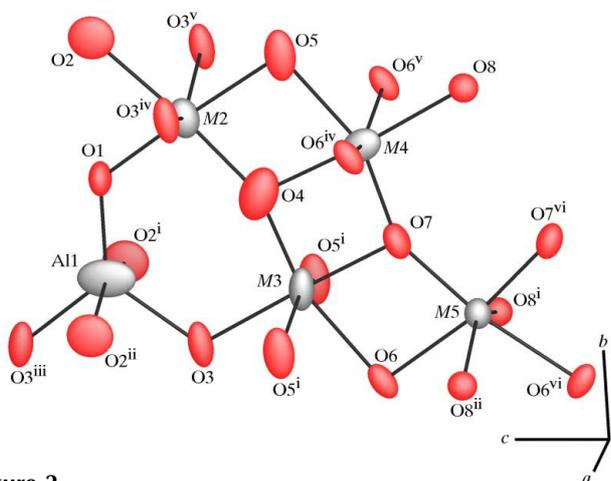


Figure 2
A displacement ellipsoid plot of the $\text{Al}_6\text{Ti}_2\text{O}_{13}$ structure. The displacement ellipsoids are drawn at the 90% probability level. [Symmetry codes: (i) $-\frac{1}{2} + x, -\frac{1}{2} + y, z$; (ii) $\frac{1}{2} + x, -\frac{1}{2} + y, z$; (iii) $x, y, 1 - z$; (iv) $\frac{1}{2} + x, \frac{1}{2} + y, z$; (v) $-\frac{1}{2} + x, \frac{1}{2} + y, z$; (vi) $x, y, -z$.]

For each octahedron, the shortest metal–oxygen distance is found for the O atoms which lie inside the double chain (Fig. 2; atoms O1, O4 and O7). These belong to only three adjacent polyhedra, whereas all other O atoms connect to four. With the exception of the octahedron formed by M2, the next shortest distances are found for the apical atoms (Fig. 2; atoms O3, O5, O6 and O8). Furthermore, all the octahedra in the double strings share edges with the nearest neighbouring octahedra, forming an edge-sharing chain $[-\text{M}2\text{O}_6-\text{M}4\text{O}_6-\text{M}3\text{O}_6-\text{M}5\text{O}_6-\text{M}3\text{O}_6-\text{M}4\text{O}_6-\text{M}2\text{O}_6-]$ of octahedra. The shortest metal–metal distance is $2.839(6) \text{ \AA}$ and this is located between M3 and M4, sharing an octahedral edge formed by O4 and O7. The shortest O...O distance of $2.449(9) \text{ \AA}$ is found between O4 and O7.

The whole $\text{Al}_6\text{Ti}_2\text{O}_{13}$ structure can be built up by the above-described double chains, as shown in Fig. 4, with the layers sharing polyhedral edges also. Channels along [100] and [010] result, whereas layers of condensed polyhedra are formed parallel to $\langle 010 \rangle$. However, it should be noted that all poly-

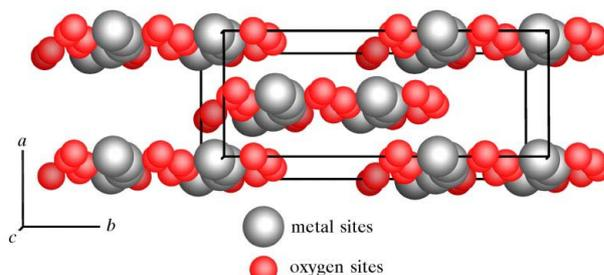


Figure 3
The atomic arrangement, viewed along [001], with the unit cell outlined.

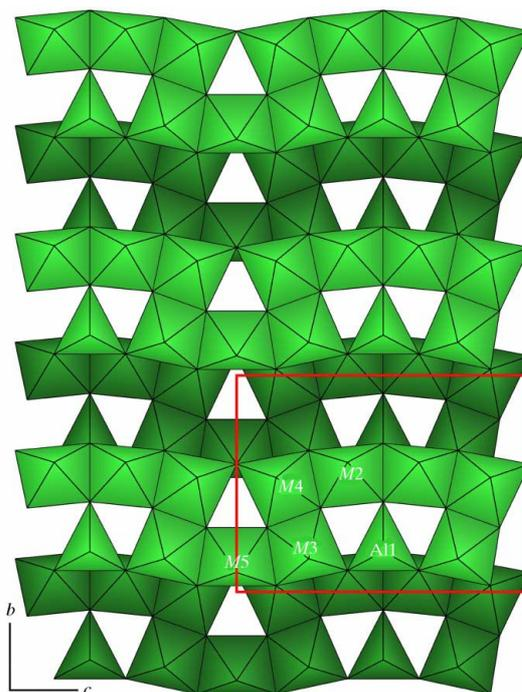


Figure 4
Polyhedral representation of the complete $\text{Al}_6\text{Ti}_2\text{O}_{13}$ structure, viewed along [100]. The unit cell is outlined.

hedra are strongly distorted. The bonding angle found in the equatorial plane of the trigonal bipyramid is either 127.8 (2) or 104.4 (3)°, which are far from the ideal value of 120°. The distorted nature of the octahedra is easily described by the divergence from the ideal 90 and 180° bonding angles found in a perfect octahedron. The ideally 90° bond angles in the M_2O_6 octahedron vary between 78.0 (2) and 103.2 (2)°, while the vertical $O_3^{IV}-M_2-O_3^V$ angle is 142.3 (4)°, which is far from 180° [symmetry codes: (iv) $\frac{1}{2} + x, \frac{1}{2} + y, z$; (v) $-\frac{1}{2} + x, \frac{1}{2} + y, z$]. Analogous distortion is seen in all other polyhedra, as well as in the similar compound β - Al_2TiO_5 (Morosin & Lynch, 1972).

Among the octahedra, we find an AlO_5 trigonal bipyramid, which is a less common coordination for Al in crystalline oxides (Santamaria-Perez & Vegas, 2003). A quick review of all Al-containing structures reported to the Inorganic Crystal Structure Database (ICSD, 2001) shows that about 4% have one or more crystallographically independent atomic sites, partly or fully occupied by Al, coordinated to five O atoms. One of the most commonly investigated structure types with AlO_5 polyhedra is the magnetoplumbite structure (Adelsköld, 1938), e.g. $SrO(Al_2O_3)_6$ (Lindop *et al.*, 1975) and $CaO(Al_2O_3)_3(Fe_2O_3)_3$ (Harder & Müller-Buschbaum, 1977), with the latter having mixed Al/Fe occupancies on all metal sites. Other examples of five-coordinated Al can be found in the families of aluminosilicates, for instance kyanite (Norton, 1925; Burnham, 1963) and andalusite (Taylor, 1929; Burnham & Buerger, 1961), which are both polymorphs of Al_2SiO_5 . Recent studies have revealed that AlO_5 units are also present in amorphous alumina (Gutierrez & Johansson, 2002), as well as in liquid alumina (Landron *et al.*, 2001).

Al and Ti have a tendency to share atomic sites, as the atomic radii of Al^{3+} and Ti^{4+} (0.53 and 0.61 Å, respectively; Shannon, 1976) are alike enough to facilitate site sharing in oxide structures. Thus, it is not unexpected that no apparent ordering exists for the crystallographically independent centres of the octahedra. Similar disorder has, for instance, been seen in studies of β - Al_2TiO_5 (Morosin & Lynch, 1972; Epicier *et al.*, 1991) which, like $Al_6Ti_2O_{13}$, is composed of strongly distorted octahedra. However, the trigonal bipyramid is, in contrast with the octahedra, exclusively occupied by Al according to the present X-ray single-crystal structure analysis. A similar situation was found in the compound $SrFe_7Al_5O_{19}$, where cation ordering happens in such a way that the bipyramids are exclusively centred by Al^{3+} (Pausch & Müller-Buschbaum, 1976).

Experimental

An appropriate sample for the structure determination of $Al_6Ti_2O_{13}$ was prepared by melting the corresponding oxides in an arc-imaging furnace followed by a 15 min soaking period immediately below the solidification point, which was indicated by a deformation of the sample surface as well as by a change in reflectivity. It should be noted that the solidification point temperature was not determined directly, but it is known from the literature (Lang *et al.*, 1952, and references therein) that equimolar melts of alumina and titania solidify between 2073 and 2133 K. The sample obtained had a flattened spherical shape with a diameter of 2–3 mm. The crushed sample was examined

using a conventional light microscope. Some parts of the sample were transparent white, while others were transparent deep blue to light blue. The Al–Ti ratio was analysed in a multitude of crystalline fragments from the $Al_6Ti_2O_{13}$ sample using an energy dispersive X-ray spectrometer (Jeol JED-2001 and JSM-6100). All selected fragments had different sizes and shapes, and every measurement gave an Al–Ti ratio of 3:1, as expected for a homogeneously synthesized globule containing a 3:2 ratio of Al_2O_3 and TiO_2 . No traces of Cu contamination from the water-cooled sample stage that was used during sample preparation with the arc-imaging furnace were found.

Crystal data

$Al_6Ti_2O_{13}$	Mo $K\alpha$ radiation
$M_r = 465.68$	Cell parameters from 23 733 reflections
Orthorhombic, $Cm2m$	$\theta = 3.2\text{--}70.9^\circ$
$a = 3.6509$ (19) Å	$\mu = 2.57\text{ mm}^{-1}$
$b = 9.368$ (5) Å	$T = 293$ (2) K
$c = 12.554$ (6) Å	Crystal fragment, light blue
$V = 429.4$ (4) Å ³	$0.13 \times 0.08 \times 0.06$ mm
$Z = 2$	
$D_x = 3.601\text{ Mg m}^{-3}$	

Data collection

Rigaku R-Axis RAPID diffractometer	1955 independent reflections
ω scans	1770 reflections with $F > 2\sigma(F)$
Absorption correction: Gaussian (<i>RAPID-AUTO</i> ; Rigaku, 2003)	$R_{int} = 0.053$
$T_{min} = 0.789, T_{max} = 0.889$	$\theta_{max} = 45.3^\circ$
4576 measured reflections	$h = -7 \rightarrow 7$
	$k = -18 \rightarrow 18$
	$l = -24 \rightarrow 25$

Refinement

Refinement on F	$\Delta\rho_{min} = -2.26\text{ e \AA}^{-3}$
$R[F^2 > 2\sigma(F^2)] = 0.074$	Extinction correction: isotropic
$wR(F^2) = 0.123$	Gaussian [Zachariasen (1967); Larson (1970), equation 22, p. 292]
$S = 1.39$	Extinction coefficient: $4(3) \times 10^2$
1995 reflections	Absolute structure: Flack (1983), 897 Friedel pairs
70 parameters	Flack parameter: 0.5 (2)
$w = 1/[\sigma^2(F) + 0.01(F)^2]$	
$(\Delta/\sigma)_{max} = 0.001$	
$\Delta\rho_{max} = 2.83\text{ e \AA}^{-3}$	

The systematic absences ($hkl: h + k = 2n, 0kl: k = 2n, h0l: h = 2n, hk0: h + k = 2n, h00: h = 2n$ and $0k0: k = 2n$) suggested $Cmmm$, $Cm2m$ and $C222$ as possible space groups. *SIR97* (Altomare *et al.*, 1999) was used with a cell setting of $P1$ to produce a set of atomic positions that were refined using the *Xtal3.7* software package (Hall *et al.*, 2000). Adding a symmetry operation of $(x + \frac{1}{2}, y + \frac{1}{2}, z)$ revealed the complete structure and determined the space group to be $Cm2m$. The non-standard setting of space group $Amm2$ was selected as it is a non-isomorphic subgroup of $Cmcm$, which is the established space group for the related compound β - Al_2TiO_5 (Austin & Schwartz, 1953). Both the refined isotropic extinction parameter (Zachariasen, 1967) and the Flack (1983) parameter have unusually large standard uncertainties, even though the determined value of each was extremely stable during the refinement, as indicated by the low $(\Delta/\sigma)_{max}$. About 3% of the reflections were affected by extinction, with a maximum correction of $y = 0.88$ for the 200 reflection (the observed structure factor is $F_{obs} = yF_{kin}$, where F_{kin} is the kinematic value). Most of the affected reflections have a y value of 0.99 or 0.98. Nevertheless, the refined extinction was deemed necessary for successfully describing this structure. The refined Flack parameter of 0.5 (2) is ambiguous, but a test using fixed Flack parameter values between 0.3 and 0.7 revealed that values within this interval have an almost non-existent influence on the final structure parameters. All that can be said from the final Flack parameter is that the crystal fragment used for diffraction is likely to contain domains of its inversion twin.

Data collection: *RAPID-AUTO* (Rigaku, 2003); cell refinement: *RAPID-AUTO*; data reduction: *RAPID-AUTO*, and *DIFDAT*, *SORTRF* and *ADDREF* in *Xtal3.7* (Hall *et al.*, 2000); program(s) used to solve structure: *SIR97* (Altomare *et al.*, 1999); program(s) used to refine structure: *CRYLSQ* in *Xtal3.7* (Hall *et al.*, 2000); molecular graphics: *DIAMOND* (Brandenburg, 2001), and *FOURR*, *SLANT* and *CONTRS* in *Xtal3.7* (Hall *et al.*, 2000); software used to prepare material for publication: *BONDLA*, *ATABLE* and *CIFIO* in *Xtal3.7* (Hall *et al.*, 2000).

Hisashi Hibino is thanked for help with the energy-dispersive X-ray diffraction measurement. STN acknowledges JSPS post-doctoral fellowship No. P03707 and SH acknowledges JSPS post-doctoral fellowship No. P03752.

Supplementary data for this paper are available from the IUCr electronic archives (Reference: SQ1191). Services for accessing these data are described at the back of the journal.

References

- Adelsköld, V. (1938). *Ark. Kemi Miner. Geol. A*, **12**, 1–9.
- Altomare, A., Burla, M. C., Camalli, M., Cascarano, G., Giacovazzo, C., Guagliardi, A., Moliterni, A. G. G., Polidori, G. & Spagna, R. (1999). *J. Appl. Cryst.* **32**, 115–119.
- Austin, A. E. & Schwartz, C. M. (1953). *Acta Cryst.* **6**, 812–813.
- Bayer, G. (1971). *J. Less Common Met.* **24**, 129–138.
- Brandenburg, K. (2001). *DIAMOND*. Version 2.1. Crystal Impact GbR, Bonn, Germany.
- Burnham, C. W. (1963). *Z. Kristallogr.* **118**, 337–360.
- Burnham, C. W. & Buerger, M. J. (1961). *Z. Kristallogr.* **115**, 269–290.
- Bursill, L. A., Hyde, B. G. & Philp, D. K. (1971). *Philos. Mag.* **23**, 1501–1513.
- Epicier, T., Thomas, G., Wohlfromm, H. & Moya, J. S. (1991). *J. Mater. Res.* **6**, 138–145.
- Flack, H. D. (1983). *Acta Cryst.* **A39**, 876–881.
- Gibb, R. M. & Anderson, J. S. (1972a). *J. Solid State Chem.* **5**, 212–225.
- Gibb, R. M. & Anderson, J. S. (1972b). *J. Solid State Chem.* **4**, 379–390.
- Gutierrez, G. & Johansson, B. (2002). *Phys. Rev. B*, **65**, 104202–104209.
- Hall, S. R., du Boulay, D. J. & Olthof-Hazekamp, R. (2000). Editors. *Xtal3.7 Reference Manual*. University of Western Australia: Lamb, Perth.
- Harder, M. & Müller-Buschbaum, H. (1977). *Z. Naturforsch. Teil B*, **32**, 833–834.
- Hyde, B. G. & Andersson, S. (1989). *Inorganic Crystal Structures*. New York: John Wiley.
- ICSD (2001). Inorganic Crystal Structure Database. Version 2004-02. FIZ-Karlsruhe. URL: <http://www.fiz-karlsruhe.de/fiz/products/icsd/welcome.html>
- Kamiya, S., Yoshimura, M. & Somiya, S. (1980). *Mater. Res. Bull.* **15**, 1303–1312.
- Landron, C., Hennet, L., Jenkins, T. E., Greaves, G. N., Coutures, J. P. & Soper, A. K. (2001). *Phys. Rev. Lett.* **86**, 4839–4842.
- Lang, S. M., Fillmore, C. L. & Maxwell, L. H. (1952). *J. Res. Natl Bur. Stand.* **48**, 298–312.
- Larson, A. C. (1970). *Crystallographic Computing*, edited by F. R. Ahmed, S. R. Hall & C. P. Huber, pp. 291–294. Copenhagen: Munksgaard.
- Lindop, A. J., Matthews, C. & Goodwin, D. W. (1975). *Acta Cryst.* **B31**, 2940–2941.
- Mazerolles, L., Bianchi, V. & Michel, D. (1994). Proceedings for ICEM 13, Paris, 17–22 July, pp. 905–906.
- Morosin, B. & Lynch, R. W. (1972). *Acta Cryst.* **B28**, 1040–1046.
- Norton, J. T. (1925). *J. Am. Ceram. Soc.* **8**, 636–639.
- Pauling, L. (1930). *Z. Kristallogr.* **73**, 97–113.
- Pausch, H. & Müller-Buschbaum, H. (1976). *Z. Naturforsch. Teil B*, **31**, 1148.
- Rigaku (2003). *RAPID-AUTO*. Version 2.12. Rigaku Corporation, Tokyo, Japan.
- Santamaria-Perez, D. & Vegas, A. (2003). *Acta Cryst.* **B59**, 305–323.
- Shannon, R. D. (1976). *Acta Cryst.* **A32**, 751–767.
- Taylor, W. H. (1929). *Z. Kristallogr.* **71**, 205–218.
- Thomas, H. A. J. & Stevens, R. (1989). *Br. Ceram. Trans. J.* **88**, 144–151.
- Yashima, M., Ishizawa, N. & Yoshimura, M. (1993). *J. Am. Ceram. Soc.* **76**, 649–656.
- Zachariasen, W. H. (1967). *Acta Cryst.* **23**, 558–564.